EUV Scattering and Flare of 10x Projection Cameras

E. M. Gullikson*[a], S. Baker[b], J. E. Bjorkholm[c], J. Bokor[a], K. A. Goldberg[a], J. E. M. Goldsmith[d], C. Montcalm[b], P. Naulleau[a], E. Spiller[b], D.G. Stearns[e], J. S. Taylor[b], J. H. Underwood[a]

[a]Lawrence Berkeley National Laboratory, Berkeley, CA 94720
[b]Lawrence Livermore National Laboratory, Livermore, CA 94551
[c]Intel, Components Research, Santa Clara, CA 95052-8126
[d]Sandia National Laboratories, PO Box 969, MS 9409, Livermore, CA 94551
[e]OS Associates, 1174 Castro St., Suite 250, Mountain View, CA 94040

ABSTRACT

Two new Schwarzschild cameras have been fabricated for the extreme ultraviolet (EUV) 10x microstepper. The surface topography of the mirrors was characterized over the full range of spatial frequencies both before and after multilayer coating. EUV scattering from the individual mirrors was measured and compared with the surface profilometry. A knife-edge test was used to directly measure the flare of the assembled cameras. The flare measured in this way is in excellent agreement with the contrast of isolated printed lines and with the point spread function of the camera as determined by EUV interferometry. The measured flare of the camera is also in good agreement with the flare calculated from the combined surface profile measurements of the individual mirrors. Consistent with the improvements made in the surface finish of the mirror substrates, a significant reduction in the flare is observed as compared with previously existing cameras.

Keywords: Extreme Ultraviolet Lithography, Flare, Light Scattering, Roughness, Power Spectral Density

1. INTRODUCTION

Scattering becomes increasingly important as the wavelength of light is reduced. For a reflective optic the total integrated scatter increases roughly as $1/\lambda^2$. The detrimental effects of scattering are: 1) a reduction in throughput due to light being lost from the camera; 2) a reduction in the image contrast by light which is redirected from bright regions of the imaged pattern into otherwise dark regions. A loss in throughput may be compensated, for example by increased exposure time. However, a reduction in the contrast degrades the image quality and is a more serious problem. The level of the scattered light in an otherwise dark region we refer to as flare. Flare reduces the exposure latitude. In addition, flare may cause the contrast to vary over the field of view if the pattern density varies, or as the edge of the field is approached. In turn, a variation in contrast will result in a variation in the printed line width.

Optical substrates for two Schwarzschild cameras have been fabricated with extremely strict tolerances on both figure and finish errors. These cameras are representative of the current state-of-the-art in optical fabrication. The substrates were coated and assembled into cameras. The multilayer coating is reported in a separate paper in these proceedings[1]. Both EUV and visible interferometry of the assembled cameras are described by Goldberg et al[2]. The imaging performance obtained with these cameras is described by Goldsmith et al[3]. The characterization of the scattering from the individual mirrors is described here along with the determination of the flare level in the assembled cameras.

2. THEORY

The scattering from a multilayer can be rather complex; however, for small scattering angles the multilayer may be regarded as a single reflecting surface. This approximation is valid for the small angles corresponding to the field of view (0.1 deg) of the Schwarzschild camera being discussed here. The scattering from a single surface may be calculated according to[4]

* Correspondence: Email: EMGullikson@lbl.gov
SPIE Proceedings Vol. 3676-94 (Mar 1999)

Downloaded From: http://proceedings.spiedigitallibrary.org/ on 03/27/2015 Terms of Use: http://spiedl.org/terms

$$\frac{1}{I_0}\frac{dI}{d\Omega}=\frac{16\pi^2}{\lambda^4}R\cdot S\cdot \mathrm{PSD}(f) \qquad (1)$$

where R is the reflectivity of the smooth surface and $S=\exp[-(4\pi\sigma/\lambda)^2]$ is the Strehl ratio. The two dimensional power spectral density (PSD) describes the surface roughness, which is assumed to be isotropic and is a function of the radial spatial frequency, $f=\sin\theta/\lambda$, where θ is the scattering angle measured from the specularly reflected beam. This expression assumes that the incident and scattered angles are small (close to the normal) and the scattering is rotationally symmetric about the reflected beam.

The effect of scattering on the image produced by a camera may be described by a scattering point spread function (PSF_{sc}). The image is calculated by convolving the PSF with the aerial image intensity calculated without scattering, but including the effects of the figure errors of the optics and the coherence of the illumination. For a single mirror, the PSF_{sc} is proportional to the angular distribution of scattering,

$$\mathrm{PSF}_{sc}(r)=\frac{1}{\rho^2}\frac{1}{I_0 R}\frac{dI}{d\Omega} \qquad (2)$$

where ρ is the distance between the mirror surface and the image plane.

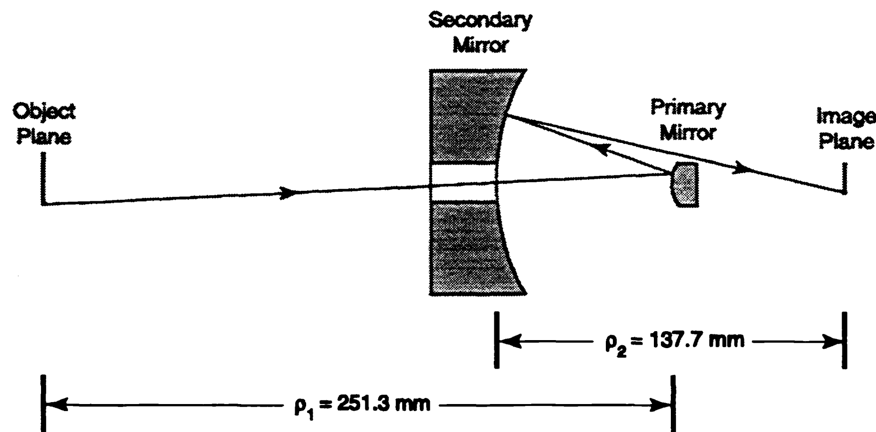

Figure 1. The 10x Schwarzschild camera.

For the Schwarzschild 10x camera consisting of two mirrors, shown in Fig. 1, the scattering point spread function is given by[5]

$$\mathrm{PSF}_{sc}(r)=S\delta(r)+\frac{16\pi^2 S}{\lambda^4\rho_2^2}\left(\mathrm{PSD}_2\left(\frac{r}{\lambda\rho_2}\right)+\alpha^2\mathrm{PSD}_1\left(\frac{\alpha r}{\lambda\rho_2}\right)\right) \qquad (3)$$

where the delta function which accounts for the specular image has been explicitly included. The first term with the beackets describes the scattering from the secondary (final) mirror with PSD_2 at a spatial frequency of $f=r/\lambda\rho_2$. The distance from the secondary mirror to the image plane is $\rho_2 = 137.7$ mm. The second term describes the scattering from the primary mirror at a

Downloaded From: http://proceedings.spiedigitallibrary.org/ on 03/27/2015 Terms of Use: http://spiedl.org/terms

spatial frequency which is scaled by $\alpha = M\rho_2/\rho_1 = 5.48$ relative to that of the secondary, where $M = 10$ is the camera magnification and $\rho_1 = 251.3$ mm is the object to primary mirror distance. The radial distance, r, in the image plane is proportional to the spatial frequency of the roughness on each of the mirrors as depicted in figure 2.

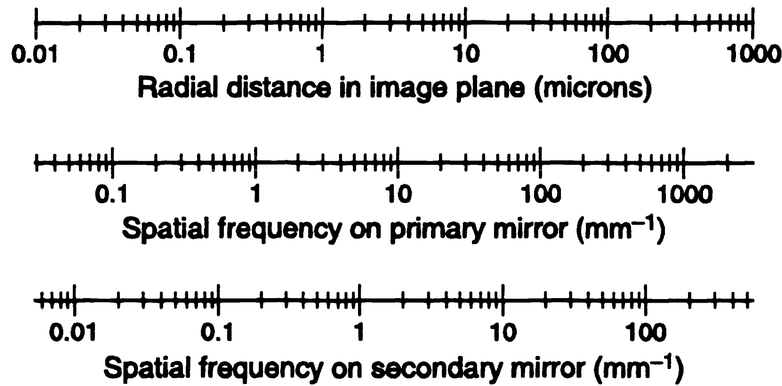

Figure 2. The radial distance in the image plane is proportional to the spatial frequency on the surface of the mirrors.

The reduction of image contrast by scattering may be seen by considering the intensity in an isolated dark line within a bright field. The aerial image intensity may be calculated by convolving the image produced in the absence of scattering with the PSF given above. The intensity in the center of the line is increased due to the tail of the PSF which extends from the bright regions of the field into the dark line. As the width of the line is reduced the intensity in the center of the line increases because of the contribution from nearby bright points. Since it is convenient to describe the effects of scattering on the image contrast by a single number, *flare* is often defined as the intensity in the center of a dark line of a specified width in a uniformly bright field. In this paper we will specify the flare for a 4 micron line. This is approximately 40 times the camera resolution and happens to correspond to a spatial frequency of about 1 mm^{-1} on the secondary mirror.

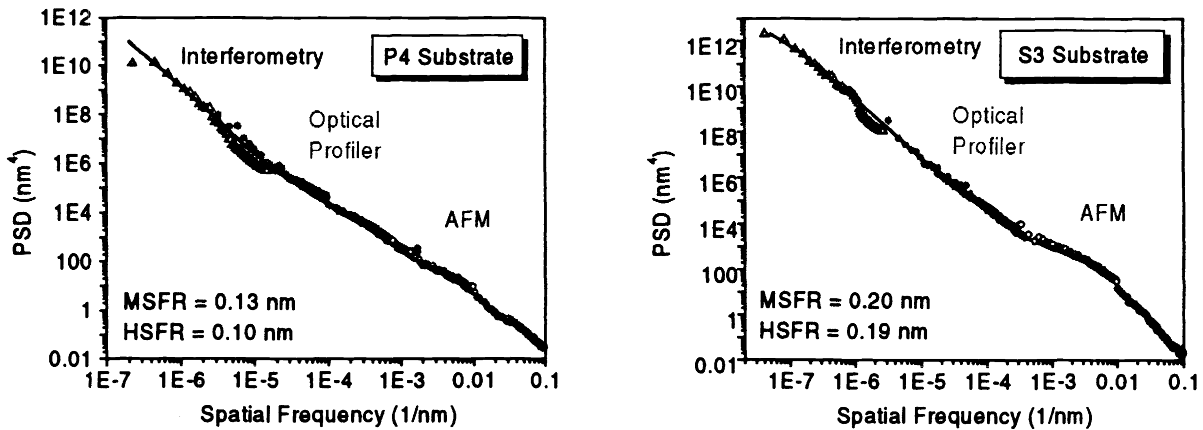

Figure 3. The measured PSDs of the substrates of the primary (P4) and the secondary (S3) mirrors of camera 2. Measurements were obtained using three different instruments. The mid-spatial frequency roughness (MSFR) and high spatial frequency roughness (HSFR) obtained by integrating the PSD is indicated for each mirror.

Downloaded From: http://proceedings.spiedigitallibrary.org/ on 03/27/2015 Terms of Use: http://spiedl.org/terms

3. CHARACTERIZATION OF THE OPTICS

It is clear from the above discussion that any calculation of scattering from a mirror surface requires a knowledge of the PSD of the surface roughness. The PSD of each of the mirrors has been measured over the range of length scales from the size of the mirror down to 10 nm. In Fig. 3, the PSDs are shown for the primary (P4) and secondary mirrors (S3) which were later assembled into camera 2. Similar measurements were obtained for the substrates of camera 1 (P3 and S2). The measurements were obtained with three separate instruments and in five locations on each mirror. The points plotted in figure 3 represent an average of the 5 locations. The solid line is a smooth curve drawn through the measurements which was used for the later calculations. The interfereometry data was obtained from the vendor. The optical profilometry was obtained with a Zygo Newview interference microscope at LLNL using both 7.5X and 40X magnifications. The AFM measurements were performed at LLNL using a Digital Instruments 5000 operated in tapping mode. AFM scans were made over both a 10 square micron and a 1 square micron field of view. The mid-spatial frequency roughness (MSFR) was calculated by integrating the PSD over the frequency range from 1 mm^{-1} to 1 μm^{-1} and can be regarded as a measure of the small angle scattering which results in flare The high spatial frequency roughness (HSFR) was calculated by integrating the PSD over the range 1 μm^{-1} to 50 μm^{-1} and can be regarded as a measure of the large angle scattering which reduces the reflectivity of the mirror. The secondary mirror, which was fabricated from Zerodur, exihibits a characteristically larger HSFR than the primary mirror which was fabricated out of fused silica.

The top surface of the mirrors was measured again by AFM after multilayer coating. As can be seen from the PSDs in Fig. 4 the coating introduces roughness in the range of spatial frequencies above about 0.005 nm^{-1}. The solid curve through the measured top surface PSD was calculated from the substrate PSD using a linear film growth model and previously determined growth parameters[5] for Mo/Si multilayer films which were deposited in the same deposition system as was used to coat these mirrors.

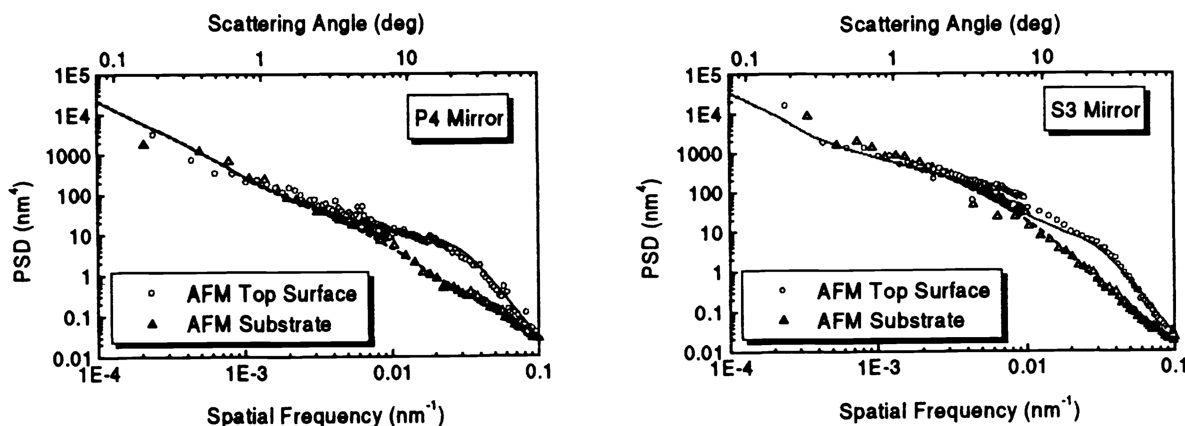

Figure 4. The PSDs determined by AFM measurements before and after Mo/Si multilayer coating. The solid line through the points for the top surface was calculated by applying a linear growth model to the measured substrate PSD.

4. SCATTERING MEASUREMENTS

4.1. The Individual Mirrors

EUV scattering was measured for each of the two secondary mirrors after they were multilayer coated. The measurements were performed at the reflectometry and scattering beamline operated by the Center for X-ray Optics at the Advanced Light Source (ALS) in Berkeley. EUV synchrotron light, at a wavelength of 13.4 nm, was used to illuminate a pinhole at a distance of 110 mm from the mirror. The pinhole was re-imaged with a magnification of unity into a channeltron detector which could be scanned in angle. The angular distribution of scattering for the two mirrors is shown in Fig. 5. The calculated angular distribution is also shown and was obtained from Eq. (1) and the measured PSDs of the coated surfaces. The single surface scattering approximation is not expected to hold for large angles and indeed the calculated curves deviate from the

Downloaded From: http://proceedings.spiedigitallibrary.org/ on 03/27/2015 Terms of Use: http://spiedl.org/terms

measurements above about 15 deg. In the case of mirror S3 the measured scattering was higher than predicted in the angular range 3 to 15 degrees. The excess scattering is consistent with the 2.5% loss in reflectivity found for this mirror. It is evident that neither the excess scattering nor the loss in reflectance for S3 could be attributed to the roughness of the substrate. Upon careful examination of the mirror a residue was found of approximately 100 nm sized particles which were not removed by the cleaning procedure prior to coating. It is estimated that scattering from these particles would account for the excess scattering and the resulting loss in reflectivity. This excess scattering should affect only the camera throughput and not the image contrast since it occurs at angles outside the field of view of the camera. At angles below 1 degree the measured scattering is in good agreement with that calculated from the measured PSDs and as will be seen the flare of the assembled camera is also consistent with the measured PSDs.

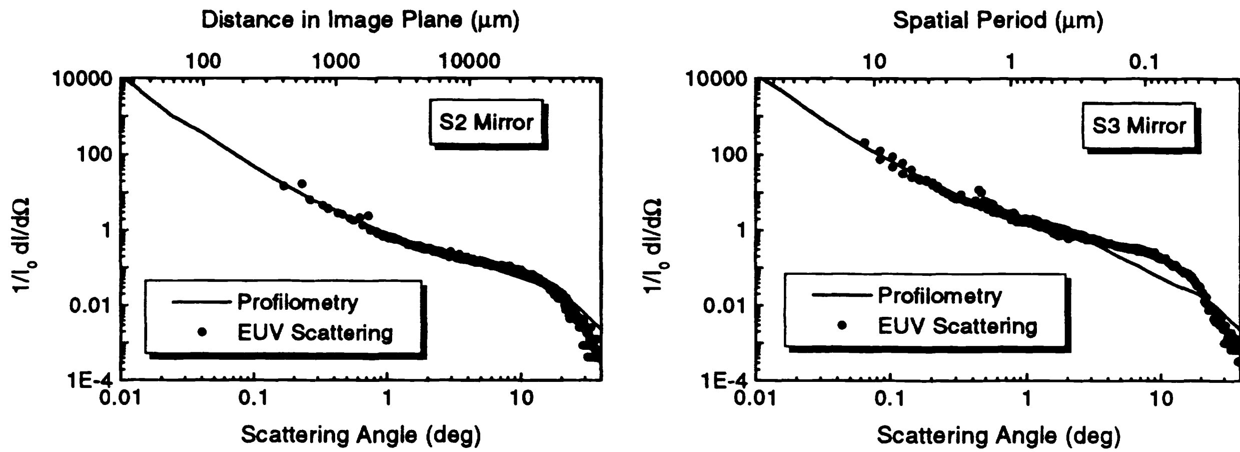

Figure 5. EUV scattering from the secondary mirrors. The solid lines are the calculated scattering for a single surface with the PSD measured for the top (coated) surface of each of the mirrors.

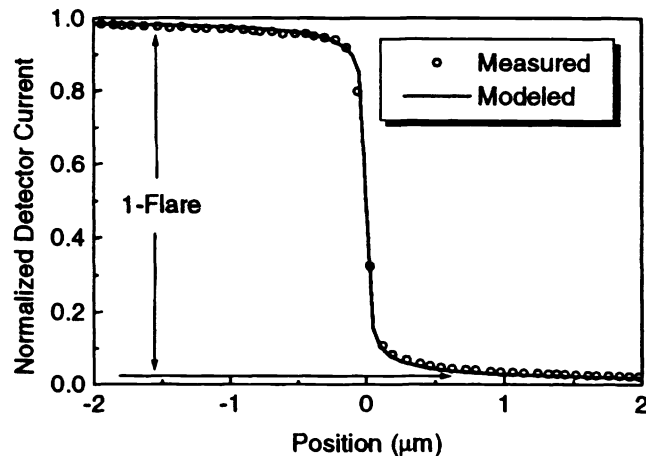

Figure 6. Knife-edge scan through the image of a 750 nm pinhole produced with camera 1. The flare is the amount of light scattered outside the image. For a 4 micron line, the width of the scan, the flare level is 4.5%. The solid line was calculated from the surface profile measurements on the individual optics of camera 1.

Downloaded From: http://proceedings.spiedigitallibrary.org/ on 03/27/2015 Terms of Use: http://spiedl.org/terms

4.2. Flare of the Camera

The mirrors were assembled into cameras and aligned. The flare of the assembled camera 1 (consisting of the P3 and S2 mirrors) was determined in three different ways. In the first test the camera was used to image a 750-nm pinhole which was illuminated with synchrotron light at the EUV Interferometry beamline at the ALS. The light passing through a 0.5-mm square aperture in the image plane was detected with a photodiode. The size of the aperture was chosen to match the field of view of the camera. With the aperture centered on the image of the pinhole, the intensity of light measured by the photodiode is the sum of the specular and scattered light. The amount of light contained in the specular image can be determined by using the edge of the aperture as a knife-edge to scan through the image of the pinhole. The results of such a scan are shown in Fig. 6 where the photodiode signal was normalized to that obtained when the aperture was centered on the image. The flare can be directly obtained from the measured scan. Choosing to specify the flare for a 4 micron line, the width of the scan in Fig. 6, the measured flare is 4.5%. This is in good agreement with calculations based on the measured surface roughness of the individual optics, shown as a solid line in Fig. 6, which would predict a flare of 4% for a 4-micron line.

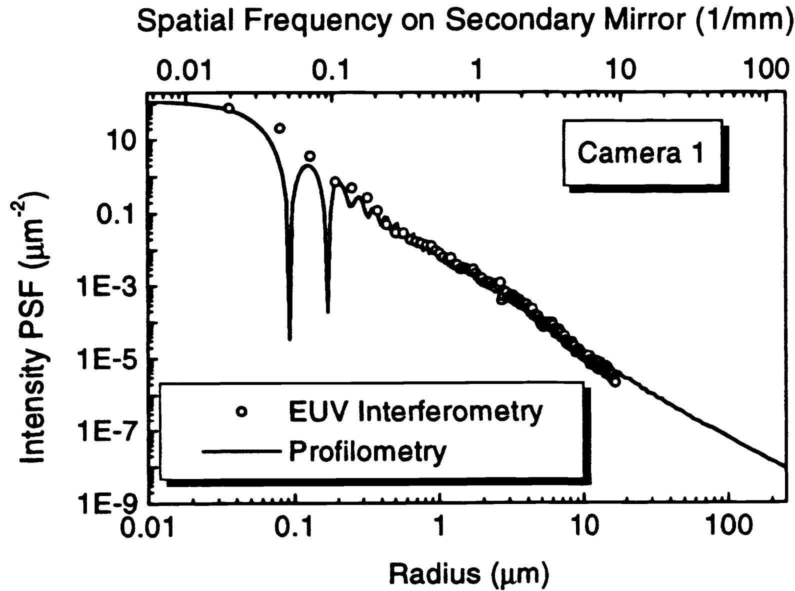

Figure 7. The Point Spread Function of camera 1 as measured by EUV interferometry is compared to that calculated from Equation (4) and the measured PSDs of the individual mirrors.

Two additional independent measurements have been performed which also put the flare level in the 4-5% range. One uses the wavefront errors determined by EUV interferometry[6] to determine the point spread function (PSF) of the camera. The wings of the PSF, which describe the level of scattering, are determined from the high frequency wavefront errors. The PSF obtained from the Fourier transform of the measured wavefront, both phase and amplitude, is shown in Fig. 7. The PSF labeled "profilometry" includes both the effects of scattering and diffraction and was calculated from

$$\mathrm{PSF}(r) = \mathrm{PSF}_{\mathrm{diff}}(r) * \mathrm{PSF}_{\mathrm{sc}}(r) \approx S \cdot \mathrm{PSF}_{\mathrm{diff}}(r) + \frac{16\pi^2 S}{\lambda^4 \rho_2^2}\left(\mathrm{PSD}_2\left(\frac{r}{\lambda\rho_2}\right) + \alpha^2 \mathrm{PSD}_1\left(\frac{\alpha r}{\lambda\rho_2}\right)\right) \qquad (4)$$

The effect of diffraction from the finite numerical aperture of the optics (NA=0.088) is described by a convolving the scattering $\mathrm{PSF}_{\mathrm{sc}}$ with the diffraction $\mathrm{PSF}_{\mathrm{diff}}$ which is the Airy function[7],

$$\mathrm{PSF}_{\mathrm{diff}}(r) = \frac{\alpha^2}{4\pi}\left(\frac{2J_1(\alpha r)}{\alpha r}\right)^2, \quad \text{where} \quad \alpha = \frac{2\pi \mathrm{NA}}{\lambda} \qquad (5)$$

Downloaded From: http://proceedings.spiedigitallibrary.org/ on 03/27/2015 Terms of Use: http://spiedl.org/terms

The normalization is such that the area of the PSF is unity integrated over the field of view. From the results shown in figure 7, it can be seen that there is a remarkable agreement between the measured and calculated PSF. A flare of 4% is obtained by integrating the measured PSF extrapolated to the size of the field of view.

Finally, the flare was measured lithographically with camera 1 installed in the Sandia 10xI system[3]. In this measurement, 4 micron lines were printed and it was found that an overexposure of 20x did not quite clear the line. This puts the flare level at somewhat less than 5%.

5. CONCLUSIONS

State-of-the-art optics for EUV lithography have been fabricated and their scattering has been fully characterized. The relationship between the optical finish of the mirror substrates and the flare of the assembled camera is clearly demonstrated. The improvements made in mirror finishing translate directly into a reduced level of flare compared with previous cameras[8]. These results are very encouraging for the success of the next generation of EUV imaging optics which will have more mirrors and an increased field of view, both of which tend to increase the level of flare.

ACKNOWLEDGEMENTS

This work was performed under the auspices of the U.S. Department of Energy. Funding was provided by the Extreme Ultraviolet Limited Liability Corporation under a Cooperative Research and Development Agreement.

REFERENCES

[1] C. Montcalm, E. Spiller, M. Wedowski, E.M. Gullikson, J.A. Folta, "Multilayer coatings of 10x projection optics for extreme-ultaviolet lithography", in *Emerging Lithographic Technologies III*, Y. Vladimirsky, Editor, Proc. SPIE 3676 *these proceedings* (1999).
[2] K.A. Goldberg, P. Naulleau, R. Gaughan, H. Chapman, J.E.M. Goldsmith, J. Bokor, "Direct Comparison of EUV and visible-light interferometries", in *Emerging Lithographic Technologies III*, Y. Vladimirsky, Editor, Proc. SPIE 3676 *these proceedings* (1999).
[3] J.E.M. Goldsmith et al., "Sub-100-nm Imaging with the EUV 10x microstepper", in *Emerging Lithographic Technologies III*, Y. Vladimirsky, Editor, Proc. SPIE 3676 *these proceedings* (1999).
[4] E.L. Church and P.Z. Takacs, "Surface Scattering," *Handbook of Optics* Vol. 1 (McGraw-Hill, 1995).
[5] D.G. Stearns, D.P. Gaines, D.W. Sweeney and E.M. Gullikson, *J. Appl. Phys.* 84, 1003-1028 (1998).
[6] K. Goldberg, P. Naulleau, E. Gullikson, J. Bokor, *to appear in the proceedings of EIPBN '99.*
[7] M. Born and E. Wolf, *Principles of Optics*, Pergamon Press, New York 1980.
[8] E.M. Gullikson, "Scattering from Normal Incidence EUV Optics" *Proceedings of the SPIE* Vol. 3331, 72-80 (1998).

Downloaded From: http://proceedings.spiedigitallibrary.org/ on 03/27/2015 Terms of Use: http://spiedl.org/terms